American Mineralogist, Volume 74, pages 18–30, 1989

Thermodynamic analysis of pyroxene-olivine-quartz equilibria in the system CaO-MgO-FeO-SiO_2

PAULA M. DAVIDSON,* DONALD H. LINDSLEY**
Department of Earth and Space Sciences, State University of New York, Stony Brook, New York 11794, U.S.A.

ABSTRACT

An internally consistent set of thermodynamic models for pyroxenes, olivine, and quartz in the CMFS system has been calibrated simultaneously with orthopyroxene cation distributions, orthopyroxene solution enthalpies, and phase equilibria for coexisting pyroxenes and coexisting pyroxene + olivine + quartz. New experiments on pyroxene + olivine + quartz equilibria constrain the models. Preferred values of model parameters are used to generate component activities that are consistent with our choice of apparent standard-state energies. These values are modified from the compilation of Helgeson et al. (1978) to fit newer experimental data and to incorporate coefficients of compressibility and thermal expansion.

Calculated geothermometers include those based on equilibria involving one, two, or three pyroxenes. Isothermal, isobaric augite solvus limbs are displaced to higher Ca contents relative to Lindsley's (1983) graphs. Calculated geobarometers include those based on assemblages of olivine + quartz + one, two, or three pyroxenes. The calculated temperature for coexisting olivine + quartz + orthopyroxene + augite + pigeonite is 818 ± 20 °C, in agreement with previous experiments; the pressure for this assemblage is given by P (in kbar) = 9.15 − 33.8X_{Mg}^{Pig}. Silica activity as determined from olivine-pyroxene exchange equilibria is shown to be a function not only of P, T, and Fe/(Fe + Mg) ratio of the assemblage, but also of the olivine (and pyroxene) Ca content, particularly for the olivine-augite exchange.

INTRODUCTION

Since Ramberg and Devore (1951) and Kretz (1961) demonstrated that the Fe-Mg ratios of coexisting pyroxenes (Pyx) and of olivine (Ol) + orthopyroxene (Opx) assemblages from igneous and metamaorphic rocks are different, Pyx and Ol have been analyzed with thermodynamic solution models for use in geothermometry and barometry (e.g., for Pyx—Wood and Banno, 1973; Saxena and Nehru, 1975; Wells, 1977; Davidson and Lindsley, 1985; for Ol—Wood and Kleppa, 1981; Davidson and Mukhopadhyay, 1984). These models have been reviewed elsewhere (e.g., Lindsley, 1983; Davidson, 1988; and references therein). As more experimental data become available and as applications of these models become more ambitious—from thermometry of granulites to predicting the phase chemistry of mantle assemblages—the need for internally consistent models becomes more apparent. Although many models for one or several of these phases have been presented, in most cases they have been calibrated independently. When such models are combined for joint application, they can give spurious results owing to incompatible choices of solution parameters. Values for excess energy parameters are highly correlated to those for end-member free-energy differences among reacting solutions. The purpose of this paper is to present an internally consistent set of models for the principal solid solutions [Opx, augite (Aug), pigeonite (Pig) and Ol] and quartz (Q) in the CaO-MgO-FeO-SiO_2 (CMFS) system. The models have been calibrated simultaneously with cation-distribution measurements, solution-enthalpy measurements, and phase-equilibrium experiments in the quaternary system and subsystems thereof. Most of the experiments are from the literature, but where necessary for our modeling, we performed new phase-equilibria experiments that help to constrain sensitive portions of the models.

THERMODYNAMIC MODELS

Solution properties

A thermodynamic solution model for quadrilateral Pyx and quadrilateral Ol was extended by Davidson (1985) from Thompson's (1969, 1970) model for nonconvergent disorder in binary Pyx. Its application to these quadrilateral solutions (ternary solutions with two of three atoms mixing on two crystallographic sites, while the third is restricted to one site only) was found successful for Pyx (Davidson and Lindsley, 1985) and Ol (Davidson and Mukhopadhyay, 1984) independently. Our assumption that these solutions can be treated as strictly quadrilateral is supported by the lack of direct observation of Ca in the Pyx M1 site and the lack of Ol with Ca in excess of (Fe + Mg) participating in Ol + Ol or Ol + Pyx ± Q

* Present address: Department of Geological Sciences, University of Illinois at Chicago, Chicago, Illinois 60680.
** To whom reprint requests should be addressed.

0003–004X/89/0102–0018$02.00

equilibria. This same model appears to fit the new expanded data set for the simultaneous calibrations.

In this model (Davidson, 1985), free energy of a quadrilateral solution (Pyx, e.g., or Ol with analogous end-members) is expressed as

$$\begin{aligned} G = {} & \Delta G^0_*[X(1 - X - Y) + Yt/2 + t^2/4] \\ & + F^0[Y(t/2 + X + Y)] \\ & + (1 - X - 2Y)\mu^0_{Fe_2Si_2O_6} + (2Y)\mu^0_{CaFeSi_2O_6} \\ & + (X)\mu^0_{Mg_2Si_2O_6} - \Delta G^0_E[Y(1 - X - Y - t/2) + t/2] \\ & + RT\left[\sum_i (X^{M1}\ln X^{M1}\gamma^{M1}) + \sum_j (X^{M2}\ln X^{M2}\gamma^{M2})\right], \end{aligned} \tag{1}$$

where energy parameters are given by $F^0 \equiv 2(\mu^0_{CaMgSi_2O_6} - \mu^0_{CaFeSi_2O_6}) + \mu^0_{Fe_2Si_2O_6} - \mu^0_{Mg_2Si_2O_6}$, $\Delta G^0_* \equiv \mu^0_{Mg(M1)Fe(M2)Si_2O_6} + \mu^0_{Fe(M1)Mg(M2)Si_2O_6} - \mu^0_{Fe_2Si_2O_6} - \mu^0_{Mg_2Si_2O_6}$, and $\Delta G^0_E \equiv \mu^0_{Fe(M1)Mg(M2)Si_2O_6} - \mu^0_{Mg(M1)Fe(M2)Si_2O_6}$; bulk composition is represented by X (or X_{Mg}) $= X_{Mg_2Si_2O_6}$, $Y = X_{Ca_2Si_2O_6}$; and the long-range order parameter is represented by $t = X^{M2}_{Fe} - X^{M1}_{Fe}$. Site excess functions for each site α are given by

$$\begin{aligned} RT\ln\gamma^\alpha_{Mg} = {} & W^\alpha_{12}[2X_{Mg}X^2_{Fe} + \tfrac{1}{2}X_{Fe}X_{Ca} + X_{Mg}X_{Fe}X_{Ca}] \\ & + W^\alpha_{21}[X^2_{Fe}(1 - 2X_{Mg}) + \tfrac{1}{2}X_{Fe}X_{Ca} - X_{Mg}X_{Fe}X_{Ca}] \\ & + W^\alpha_{13}[2X_{Mg}X^2_{Ca} + \tfrac{1}{2}X_{Fe}X_{Ca} + X_{Mg}X_{Fe}X_{Ca}] \\ & + W^\alpha_{31}[X^2_{Ca}(1 - 2X_{Mg}) + \tfrac{1}{2}X_{Fe}X_{Ca} - X_{Mg}X_{Fe}X_{Ca}] \\ & + W^\alpha_{23}(-\tfrac{1}{2}X_{Fe}X_{Ca} - X^2_{Fe}X_{Ca} + X_{Fe}X^2_{Ca}) \\ & + W^\alpha_{32}[-\tfrac{1}{2}X_{Fe}X_{Ca} + X^2_{Fe}X_{Ca} - X_{Fe}X^2_{Ca}] \end{aligned}$$

$$\begin{aligned} RT\ln\gamma^\alpha_{Fe} = {} & W^\alpha_{12}[X^2_{Mg}(1 - 2X_{Fe}) + \tfrac{1}{2}(X_{Mg}X_{Ca}) - X_{Mg}X_{Fe}X_{Ca}] \\ & + W^\alpha_{21}[2X^2_{Mg}X_{Fe} + \tfrac{1}{2}X_{Mg}X_{Ca} + X_{Mg}X_{Fe}X_{Ca}] \\ & + W^\alpha_{13}[X_{Mg}X^2_{Ca} - X^2_{Mg}X_{Ca} - \tfrac{1}{2}X_{Mg}X_{Ca}] \\ & + W^\alpha_{31}[X^2_{Mg}X_{Ca} - X_{Mg}X^2_{Ca} - \tfrac{1}{2}X_{Mg}X_{Ca}] \\ & + W^\alpha_{23}[2X_{Fe}X^2_{Ca} + \tfrac{1}{2}X_{Mg}X_{Ca} + X_{Mg}X_{Fe}X_{Ca}] \\ & + W^\alpha_{32}[X^2_{Ca}(1 - 2X_{Fe}) + \tfrac{1}{2}X_{Mg}X_{Ca} - X_{Mg}X_{Fe}X_{Ca}] \end{aligned} \tag{2}$$

$$\begin{aligned} RT\ln\gamma^\alpha_{Ca} = {} & W^\alpha_{12}[X_{Mg}X^2_{Fe} - X^2_{Mg}X_{Fe} - \tfrac{1}{2}X_{Fe}X_{Mg}] \\ & + W^\alpha_{21}[X^2_{Mg}X_{Fe} - X_{Mg}X^2_{Fe} - \tfrac{1}{2}X_{Mg}X_{Fe}] \\ & + W^\alpha_{13}[X^2_{Mg}(1 - 2X_{Ca}) + \tfrac{1}{2}X_{Mg}X_{Fe} - X_{Mg}X_{Fe}X_{Ca}] \\ & + W^\alpha_{31}[2X^2_{Mg}X_{Ca} + \tfrac{1}{2}X_{Mg}X_{Fe} + X_{Mg}X_{Fe}X_{Ca}] \\ & + W^\alpha_{23}[X^2_{Fe}(1 - 2X_{Ca}) + \tfrac{1}{2}X_{Mg}X_{Fe} - X_{Mg}X_{Fe}X_{Ca}] \\ & + W^\alpha_{32}[2X^2_{Fe}X_{Ca} + \tfrac{1}{2}X_{Mg}X_{Fe} + X_{Mg}X_{Fe}X_{Ca}], \end{aligned}$$

where the superscripts α are omitted from mole-fraction terms for simplicity; subscripts on W terms represent Mg (1), Fe (2), and Ca (3). Since we do not consider any Ca on the M1 site in this model, W_{13}, W_{31}, W_{23}, and W_{32} pertain to the M2 site only and their superscripts are hereafter omitted. Also because the only mixing considered on both M1 and M2 sites is Fe-Mg and because no asymmetry in Fe-Mg mixing is required, W^{M1}_{12} $(=W^{M1}_{21})$ and W^{M2}_{12} $(=W^{M2}_{21})$ are hereafter abbreviated as W^{M1} and W^{M2}, respectively.

Site occupancies X^{M1}_i and X^{M2}_j, i = Mg, Fe; j = Mg, Fe, Ca are found from requiring that free energy be minimized with respect to variations in cation distribution:

$$\begin{aligned} dG/dt = 0 = {} & \Delta G^0_*(Y + t)/2 + F^0(Y/2) - \Delta G^0_E(1 - Y)/2 \\ & + W_{13}[Y(-\tfrac{1}{2} + t/2 - X + 2Y)] \\ & + W_{31}[Y(-\tfrac{1}{2} - t/2 + X - 2Y)] \\ & + W_{23}[Y(3/2 + t/2 - X - 2Y)] \\ & + W_{32}[Y(-\tfrac{1}{2} - t/2 + X + 2Y)] \\ & + W_{12}[(\tfrac{1}{2} - t/2 - X - Y)/2] \\ & + W_{12}[(\tfrac{1}{2} - t/2 + X)/2] \\ & + (\tfrac{1}{2})RT\ln[(X^{M1}_{Mg}X^{M2}_{Fe})/(X^{M1}_{Fe}X^{M2}_{Mg})]. \end{aligned} \tag{3}$$

The notation for energy parameters is adopted from Davidson (1985).

End-member properties

Helgeson et al. (1978) presented a thermochemical model for α-quartz and β-quartz that we use here. No other silica polymorphs are considered. Apparent standard-state energies are also adapted from Helgeson et al., with modifications to avoid the apparent stability of forsterite + Q and to optimize the fit to various phase equilibria. As an example, our revision based on the reaction fayalite + Q = ferrosilite is outlined below.

The relations among Ol + Q and Pyx are very tightly controlled by the experiments of Bohlen et al. (1980) on the reaction

$$Fe_2SiO_4 + SiO_2 = Fe_2Si_2O_6.$$

Their experiments are so closely bracketed that only very limited ranges in the values of the free-energy differences are possible. In order to update the values of Helgeson et al. (1978) to comply with these newer experiments, we used the following thermochemical data for fayalite and ferrosilite with the Helgeson et al. Q model and determined a new value for apparent free energy of ferrosilite. Using the 298-K, 1-bar free-energy value for fayalite of Robie et al. (1982), we refitted their heat-capacity data to the simpler Maier-Kelley formula for compatibility with the equations of Helgeson et al. The entropy of ferrosilite is that of Anovitz (pers. comm., 1984). Table 1 gives the sources of coefficients of compressibility and thermal expansion. We then extracted the apparent free energy of formation of ferrosilite by least-squares fit to the experimental data of Bohlen et al. (1980).

We chose to adopt the approach of Helgeson et al. (1978) in using apparent free energies (standard state of reference elements remains at 298 K, 1 bar) rather than "true" free energies (standard state of reference elements is evaluated at P and T) for several reasons. First, as Helgeson et al. pointed out, the reference states cancel when reactions are considered inasmuch as *differences* in free energy are important. Second, values of "true" free

Table 1. Apparent standard-state free energies

	ΔG_f° (J)	S_{298}	A	B	C	$V_{298.15,1}$	α	β
OEn	−76 843.344	132.59933	206.12476	5.4865×10^{-2}	5.3103×10^{6}	6.2592	43.8×10^{-6}	0.93×10^{-6}
Ref.	1	1	1	1	1	7	13	3
CEn	−70 732.644	136.73167	206.12476	5.4865×10^{-2}	5.3103×10^{6}	6.35674*	43.8×10^{-6}	0.93×10^{-6}
Ref.	4	4				4		
Δ†	6 110.7	4.13234				0.09754		
Ref.	4	4				4		
OFs	−20 262.126	191.61674	232.9927	3.0405×10^{-2}	6.463×10^{6}	6.6016	39.3×10^{-6}	0.99×10^{-6}
Ref.	11	11	11	11	11	7	5	16
CFs	−18 222.126	193.31284	232.9927	3.0405×10^{-2}	6.463×10^{6}	6.6265*	39.3×10^{-6}	0.99×10^{-6}
Ref.	6	6				6		
Δ†	2 040.0	1.6961				0.0249		
Ref.	6	6				6		
Di	−143 327.1	143.0928	221.20808	3.2803×10^{-2}	6.5856×10^{6}	6.609	33.3×10^{-6}	29.8×10^{-6}
Ref.	7	7	7	7	7	7	2	8
ODi	−104 267.2	160.3876	221.20808	3.2803×10^{-2}	6.5856×10^{6}	6.74654*	33.3×10^{-6}	29.8×10^{-6}
Ref.	4	4				4		
Δ†	−39 060.	−17.295				−0.1375		
Ref.	4	4				4		
Hd	−105 795.	170.2888	229.32504	3.4183×10^{-2}	6.2802×10^{6}	6.827	29.8×10^{-6}	0.833×10^{-6}
Ref.	6	7	7	7	7	7	2	9
OHd	−95 213.	167.1016	229.32504	3.4183×10^{-2}	6.2802×10^{6}	6.8931	29.8×10^{-6}	0.833×10^{-6}
Ref.	6	6				6		
Δ†	−10 582.	3.1872				−0.0661		
Ref.	6	6				6		
Fo	−72 297.264	94.09816	155.72597	2.2055×10^{-2}	4.0488×10^{6}	4.379	$40. \times 10^{-6}$	0.775×10^{-6}
Ref.	6	17	18	18	18	7	19	10
Fa	−19 848.896	151.00056	149.1847	4.2886×10^{-2}	2.4811×10^{6}	4.639	$31. \times 10^{-6}$	0.774×10^{-6}
Ref.	14	14	14	14	14	7	19	12
Mo	−108 776.5	110.4576	154.05488	2.2343×10^{-2}	3.3472×10^{6}	5.147	$33. \times 10^{-6}$	0.82×10^{-6}
Ref.	7	7	7	7	7	7	19	19
Ks	−87 452.316	138.9088	150.78425	3.2758×10^{-2}	2.5634×10^{6}	5.277	28.5×10^{-6}	0.8195×10^{-6}
Ref.	6	6	6	6	6	15	6	6

$$\mu^\circ = \Delta G_f^\circ - S_{298}(T - 298.15) + A[T - 298.15 - T\ln(T/298.15)] + [C - BT(298.15)^2][(T - 298.15)^2]/[2T(298.15)^2] + [V_{298.15,1}(1 + \alpha(T - 298.15))][1 + \beta(P - 1) - \tfrac{1}{2}\beta(P^2 - 1)]$$

Note: References are as follows: (1) Day et al., 1985. (2) Cameron et al., 1973. (3) Weidner and Vaughan, 1982. (4) Davidson et al. (1988). (5) Sueno et al., 1976. (6) This work. (7) Helgeson et al., 1978. (8) Levien et al., 1979. (9) Kandelin and Weidner, 1987. (10) Hazen, 1976. (11) Anovitz, personal communication, 1985. (12) Yagi et al., 1975. (13) Smyth, 1973. (14) This work; Maier-Kelley polynomial fit to data of Robie et al., 1982. (15) Mukhopadhyay and Lindsley, 1983. (16) Bass and Weidner, 1984. (17) Robie et al., 1982b. (18) This work; Maier-Kelley polynomial fit to data in 17. (19) Lager and Meagher, 1978.

* Actually $V(\text{CEn}) = V(\text{OEn}) + 0.09754P$. This is very closely approximated by $V_{298.15,1}(\text{CEn}) = 6.35674$ and $\alpha(\text{OEn}) = \alpha(\text{CEn})$, $\beta(\text{OEn}) = \beta(\text{CEn})$. The same applies to other end-members.

† $\Delta \equiv \mu^\circ(\text{clino}) - \mu^\circ(\text{ortho})$.

energies are not yet available for some of the end-members we consider; such free energies must be extracted from the data through our model. Because we can only extract differences in free energy, it seems more realistic to express the results as apparent free energies.

Several thermodynamic databases now being developed employ "true" free energies. Our model for component activities should be compatible with the newer databases if they produce the same end-member difference energies (i.e., fit the same end-member equlibria). This is possible if the following *caveats* are observed:

1. Within each solid solution (Opx, Cpx and Ol), the most important parameter is the departure of the four end-member components (abbreviated as MgMg, FeFe, CaMg, and CaFe) from coplanarity as measured by our parameter F^0, where $F^0 \equiv 2(\mu^0_{\text{CaMg}} - \mu^0_{\text{CaFe}}) + (\mu^0_{\text{FeFe}} - \mu^0_{\text{MgMg}})$. Thus one should be able to substitute "true" free energies for any three end-members *so long as the free energy adopted for the fourth* maintains the value for F^0 predicted by our model. This is assuming, of course, that the values predicted for departure from coplanarity, F^0, lie within the uncertainty of any independent measures of them.

2. For relations between two or more phases, it is essential to maintain the *differences* between corresponding pairs of end-members. Most likely this will be possible within experimental uncertainty, as is illustrated schematically in Figure 1. As can be seen from that figure, at most one can pin only three end-members of one phase to the preferred free-energy values of the database; the others must be adjusted to allow for the differences required by our model for coexisting subconsolute phases. In the example, the preferred free-energy values for Di, CEn, and CFs have been used; the value for Hd is then controlled by the value for F^0, and those for Ol end-members are determined by the differences required by

the model. In this example, all the "revised" free energies fall within the uncertainties of the values within the database.

3. The relations between Ol + Q and Pyx are very tightly constrained by the experiments of Bohlen et al. (1980). It should be possible to use any set of free energies for orthoferrosilite, fayalite, and Q that is compatible with the experiments, but we strongly urge use of our values to ensure internal consistency in any calculations.

Experimental constraints

Previous studies

Cation distributions in natural Opx that were annealed at several different temperatures have been measured by Mössbauer spectroscopy (Saxena and Ghose, 1971; Besancon, 1981) and by single-crystal X-ray diffraction (Domeneghetti et al., 1985; Sykes and Molin, 1986). The two more recent studies were not used for parameter evaluation, because the reported Fe-Mg cation distributions are not directly comparable. For refinements, the total (Fe + Mg) site occupancies were normalized so as to completely fill both M sites, whereas the other data have been normalized so that (Fe + Mg + Ca) completely fill the M sites.

Cation distributions have also been measured in Cpx, both synthetic and natural, with a variety of techniques. However, we have not used any of those measurements to calibrate energy parameters, because of the following problems. Owing to the difficulties of interpreting the Mössbauer spectra in Ca-bearing Pyx (Dowty and Lindsley, 1973), the work of Saxena et al. (1974) has been omitted from the data set. Davidson and Lindsley (1985) found that the X-ray structure refinements of cation distributions for Mull Pig (Brown et al., 1972) yield results that are inconsistent with phase-equilibria models for Cpx, and those for Aug (McCallister et al., 1976) are too Ca-rich to provide much leverage on models for Fe-Mg intracrystalline exchange.

Solution enthalpies of Cpx in the $Mg_2Si_2O_6$-$Ca_2Si_2O_6$ join and of orthoenstatite were measured by Holland et al. (1979). For the $Mg_2Si_2O_6$-$Fe_2Si_2O_6$ join, Chatillon-Colinet et al. (1983) measured synthetic Opx solution enthalpies at 750 °C. Synthesis conditions were 1120 °C and 20 kbar; as noted by Davidson and Lindsley (1985), the positive deviations from ideality recorded in these measurements are more consistent with a high-temperature signature, rather than with a temperature of 750 °C where cation ordering is still measurable. Accordingly, the solution-enthalpy values are treated as reflecting the synthesis conditions.

Phase-equilibria experiments within the Pyx quadrilateral are listed in Davidson and Lindsley (1985). Most of them come from Lindsley's (1983) high-pressure experiments and Lindsley and Andersen's (1983) low-pressure experiments for coexisting Aug and Opx or Pig. For the Fe-free join, we incorporate the model by Davidson et al. (1988) for thermodynamic properties of Opx and Cpx. The Davidson et al. (1988) revision of Carlson and Lindsley's (1988) model is preferable as a starting point for quadrilateral models because, unlike its precursor, it avoids the metastable reaction whereby Pig breaks down to the *higher*-temperature assemblage Aug + Opx, which interferes with the high-temperature *production* of Pig from Aug + Opx in the quadrilateral. As is Carlson and Lindsley's model, the model of Davidson et al. is formally similar to that presented by Lindsley et al. (1981) but is based on new phase-equilibria experiments (Carlson, 1986a, 1986b; Nickel and Brey, 1984) in addition to those available to Lindsley et al.—which included solution enthalpies (Holland et al., 1979) and phase equilibria (Lindsley and Dixon, 1976; Mori and Green, 1975, 1976; Nehru and Wyllie, 1974; Schweitzer, 1982; Warner and Luth, 1974). Unlike Davidson and Lindsley's (1985) method for quadrilateral modeling, we solve for the Mg-free join simultaneously with the Ca-free join and incorporate experiments in the CFS subsystem, FMS subsystem, and CMFS system in addition to the quadrilateral subsystem.

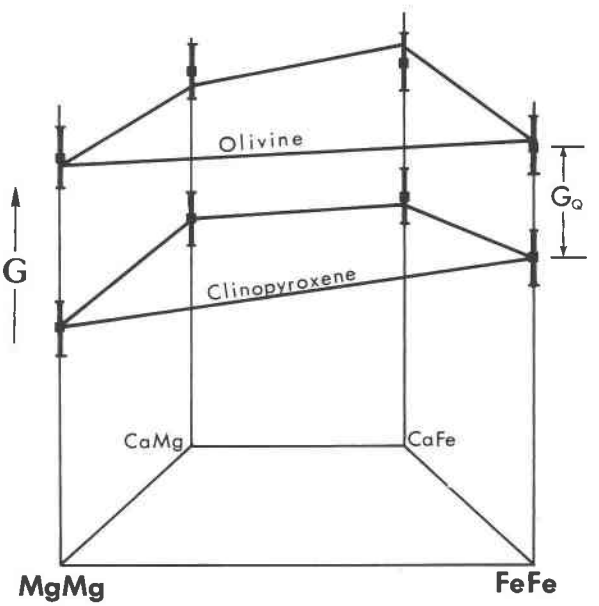

Fig. 1. Schematic free energy vs. composition relations among quadrilateral standard states. At this P and T, clinoferrosilite is in equilibrium with fayalite + Q. Heavy square superimposed on thickened range of G values indicates "preferred" value of free energy at P and T for the database in use. G_Q is the free energy of Q.

Ol + Pyx ± Q equilibria have been studied in several subsystems. Adams and Bishop's (1982) and (1986) results were reserved as a test of model parameters. Their (1982) experiments on the Ca content of Ol saturated with two Pyx in the CMS subsystem constrain the Ol model and free-energy differences between Fe-free Ol and Pyx end-members, when combined with a model such as Carlson and Lindsley's (1988) for Fe-free Pyx. Our model reproduces the measured Ca_2SiO_4 content in their Fe-free Ol to within 0.15 mol%, in all cases. Experimental data on an Fe-bearing compositions (Adams and Bishop, 1986)

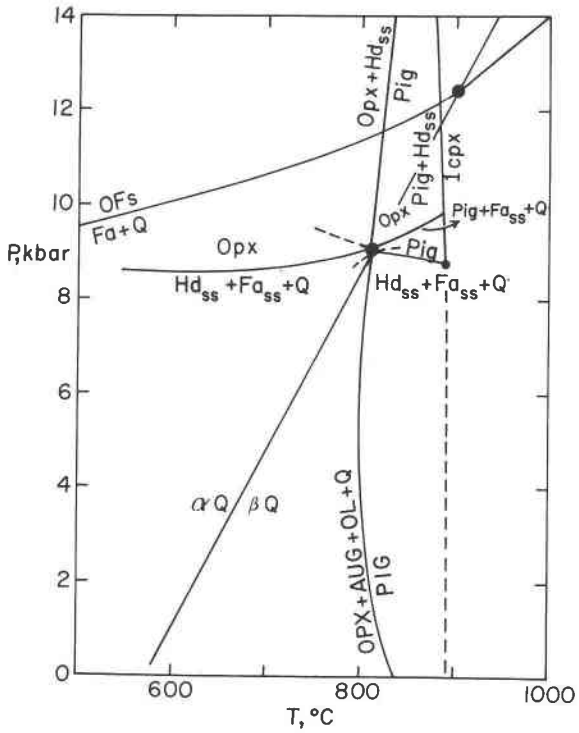

Fig. 2. Petrogenetic grid for reactions in the CFS subsystem. Also shown is the CMFS univariant reaction Aug + Opx + Ol + Q = Pig. Abbreviations: OFs, orthoferrosilite; Fa, fayalite; Hd, hedenbergite; ss, solid solutions.

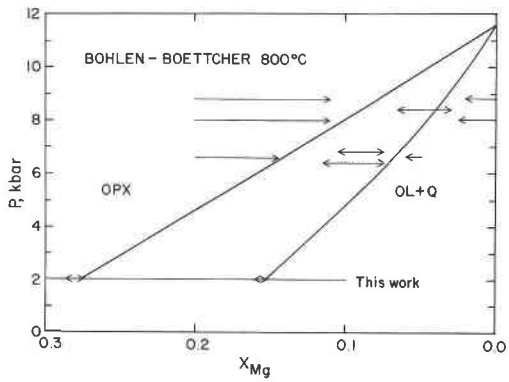

Fig. 3. *P-X* section for the join $Mg_2Si_2O_6$-$Fe_2Si_2O_6$ at 800 °C. Bohlen and Boettcher's (1981) experiments and our new experiments at 2 kbar are shown by arrows indicating direction and extent of reaction. Solid curves are calculated with the model.

for the same reactions are not accurately predicted by our model when the pressure is less than 30 kbar. Lindsley and Munoz (1969) and Bohlen and Boettcher (1981) provided experimental constraints on Ol + Q + Cpx equilibria in the CFS subsystem and on Ol + Q + Opx in the FMS subsystems, respectively. Preliminary optimization of solution parameters with these data helped to identify two critical areas for further experiments that we report below.

New experiments

Because Mg-free olivines of Ol + Q + Cpx assemblages on the $Fe_2Si_2O_6$-$CaFeSi_2O_6$ join contain very little Ca, additional evidence was needed to constrain the maximum pressure to which calcic, Mg-free Ol is stable in the presence of Q. Virginia Haniford (pers. comm., 1986) found that at 10 kbar and 800 °C, the assemblage Ol (X_{Ca} = 0.004) + Q persists in the presence of Opx (X_{Ca} = 0.036). This implies that the invariant point for coexisting Mg-free Ol, Opx, Pig, Aug, and Q lies below 10 kbar (see Fig. 2).

In the CMFS system, this five-phase assemblage is univariant. Lindsley and Grover (1980) found that it is also nearly isothermal, at about 825 °C, as our model bears out (as shown in Fig. 2). However, the compositions of Opx and Ol in this assemblage at 825 °C and 2 kbar appeared inconsistent with the trend determined by Bohlen and Boettcher (1981) in higher-pressure equilibria; the compositions of both are too Fe-rich. The Opx and Ol Fe/(Fe + Mg) ratios in the univariant assemblage are quite similar to those from Bohlen and Boettcher's Ca-free Ol + Opx + Q experiments at similar temperatures and higher pressures, implying that Fe/(Fe + Mg) ratios in coexisting Opx and Ol exhibit little pressure dependence between 2 and 6 kbar (or that Ca destabilizes Ol and Opx equally). We therefore tested the unlikely loss of pressure dependence with new experiments (listed in Table 2): synthetic Ca-free Opx and Ol were reacted in

Table 2. Experimentally determined equilibria among CMFS pyroxenes, olivines, and quartz

Starting material*	*P* (kbar)	*T* (°C)	Duration d	Duration h	Products Cpx	Pig	Opx	Ol (+ Q)
A	2	750	222	3	$Wo_{37.5}En_{18.5}$	—	$Wo_4En_{22.5}$	$Fa_{87}Fo_{12}$
B	1	800	111	7	$Wo_{37}En_{19.5}$	—	$Wo_{3\pm1}En_{24.5}$	$Fa_{83.7}Fo_{15.3}$
C	2	825	54	18	$Wo_{37.5}En_{20}$	Wo_9En_{22}	Wo_4En_{25}	$Fa_{86.8}Fo_{12.5}$
D	7	830	13	23	present	$Wo_{11}En_9$	$Wo_{4.6}En_{9.7}$	$Fa_{93.8}Fo_5$
E	7	830	13	23				
F	2	800	36	8	—	—	Wo_0En_{28}	$Fa_{84.3}Fo_{15.7}$
G	2	800	29	14				

* A: $Wo_{25}(Fs_{75}En_{25})_{75}$ (Cpx) (1 phase). B: Mechanical mix of $Fs_{75}En_{25}$ (Opx), $Wo_{50}(Fs_{75}En_{25})_{50}$ (Cpx). C: Mechanical mix of $Fs_{75}En_{25}$ (Opx), $Wo_{40}(Fs_{75}En_{25})_{60}$ (Cpx). D: Mechanical mix of $Wo_{25}(Fs_{75}En_{25})_{75}$ (Cpx) + Fa_{100} + Q + Opx seeds; bulk composition = $Wo_{10}(Fs_{92}En_8)_{90}$. E: Mechanical mix of $Wo_{15}(Fs_{92}En_8)_{85}$ (Cpx) + $Fs_{92}En_8$ (Opx) + $Fa_{92}Fo_8$ + Q; bulk composition = $Wo_{10}(Fs_{92}En_8)_{90}$. F: $Fs_{80}En_{20}$ (Opx) + $Fa_{92}Fo_8$ + Q; bulk composition = $Fs_{83}En_{17}$. G: $Fs_{70}En_{30}$ (Opx) + $Fa_{83}Fo_{17}$ + Q; bulk composition = $Fs_{80}En_{20}$.

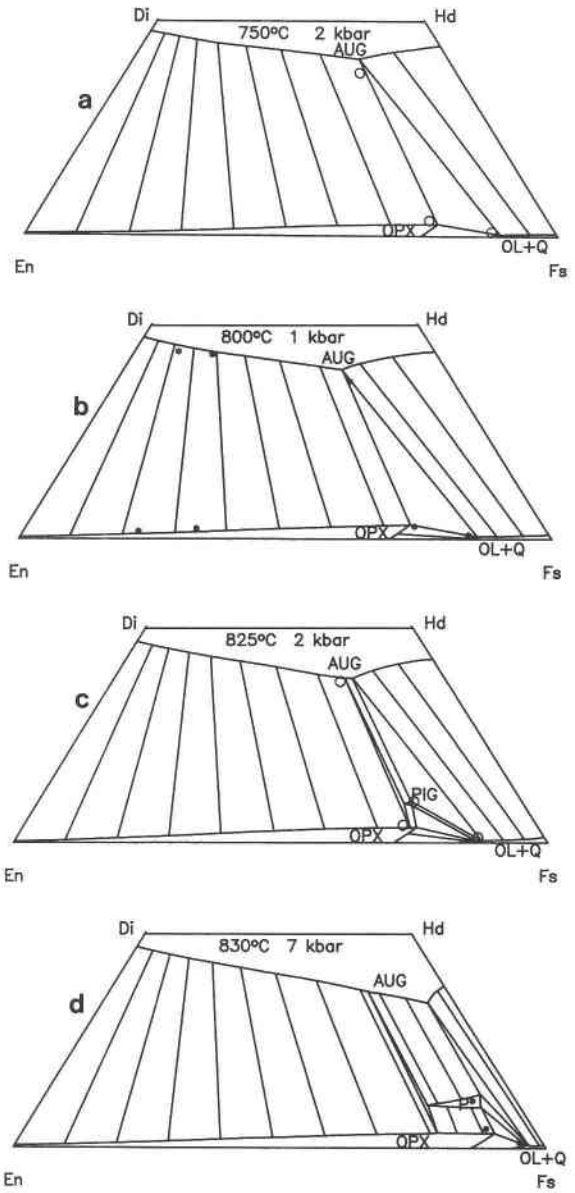

Fig. 4. Isothermal, isobaric projections of CMFS phase equilibria on the Pyx quadrilateral at several P, T conditions: **(a)** 725 °C, 2 kbar; **(b)** 800 °C, 1 kbar; **(c)** 825 °C, 2kbar; **(d)** 830 °C, 7 kbar. Experiments from Table 2 are plotted as circles and asterisks. End-members: Di, diopside; Hd, hedenbergite; Fs, ferrosilite; En, enstatite.

the presence of silica to bracket coexisting compositions at 800 °C and 2 kbar. Experiments were carried out in cold-seal pressure vessels with water as the pressure medium, buffered under FMQ conditions. Run products were analyzed with the electron microprobe, yielding $X_{Mg}^{Opx} = 0.279$, $X_{Mg}^{Ol} = 0.157$. These results are shown along with Bohlen and Boettcher's higher-pressure, 800 °C experiments in Figure 3.

Additional unpublished experiments made in Lindsley's laboratory on CMFS Pyx coexisting with Ol + Q were critical to simultaneous model calibration. Run conditions, reactants, and products are listed in Table 2. The 1- and 2-kbar experiments were performed under similar conditions as the Ca-free runs; the 7-kbar experiments were carried out in a piston-cylinder apparatus. Resulting phase compositions are given in Table 2 and plotted in Figures 4a–4d. The low-pressure runs are not reversed; however, they show upper limits of X_{Fe} in Opx and lower limits of X_{Mg} in Aug. Ol composition trends show an increase in X_{Mg} with increasing temperature and decreasing pressure, as expected from previous work (e.g., Bohlen and Boettcher, 1981).

TABLE 3. Experimental constraints employed in model calibration

Experiments	Reference
Orthopyroxene cation distributions	Saxena and Ghose (1971) Besancon (1981)
Orthopyroxene solution enthalpy	Chatillon-Colinet et al. (1983)
FMS phase equilibria	Bohlen and Boettcher (1981) This report
CFS phase equilibria	Lindsley and Munoz (1969) Lindsley (1983) Haniford (pers. comm.)
CMFS phase equilibria	Mori (1978) Podpora and Lindsley (1979) Lindsley and Grover (1980) Turnock and Lindsley (1981) Fonarev and Graphchikov (1982) Lindsley and Andersen (1983) Lindsley (1983) Lindsley (pers. comm.)

Model calibration

Experimental data were used to constrain model parameters with a nonlinear least-squares technique, as described by Davidson and Lindsley (1985), in which the model fit to experimentally bracketed compositions is iteratively improved until desired convergence is obtained. The major difference between the previous and present regression treatments is that the entire set of 129 experiments, listed in Table 3, is employed simultaneously in cyclic refinements of energy parameters. Variations of end-member enthalpy differences between Ol and Cpx, and in the Opx energy parameter W_{23} ($=W_{32}$, describing nonideal Fe-Ca mixing within the M2 site), were made externally to the regression program, because high correlations to other energy parameters prevented their simultaneous evaluation with the remaining 22 energy parameters.

The CMS two-olivine experiments of Adams and Bishop (1985) and CMFS two-olivine experiments of Davidson and Mukhopadhyay (1984) were employed in a separate nonlinear least-squares refinement of the Ol solution parameters. The final values are given in Table 4. We prefer the simpler, T-independent form of the parameters W_{13} and W_{31} (describing nonideal Mg-Ca mixing within the M2 site) for Ol rather than the parameters presented

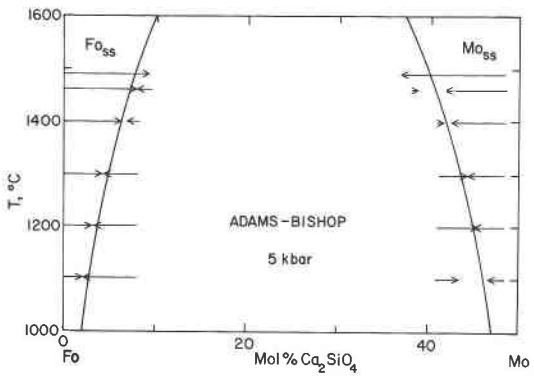

Fig. 5. T-X section for the join Mg_2SiO_4-$MgCaSiO_4$ at 5 kbar. Adams and Bishop's (1985) experiments are shown by arrows; the solid curve is calculated with our model. End-members: Fo, forsterite; Mo, monticellite.

by Adams and Bishop; the fit to their experiments is acceptable at all conditions except 5 kbar and 1490 °C (shown in Fig. 5), which is above the solidus for the two-olivine assemblage. In order to ensure compatibility with solution models for Fe-Mg-Ti oxides by David J. Andersen (pers. comm., 1987), we adopted the maximum value for ΔG^0_2 (7000 J) that is still consistent with olivine-ilmenite exchange equilibria. This value for ΔG^0_2 in turn constrains the value for W_{23} ($=W_{32}$, describing nonideal Fe-Ca mixing within the M2 site) to be the minimum (21560 J) that is compatible with two-olivine equilibria in both the $(Ca,Fe,Mg)_2SiO_4$ ternary and $(Ca,Fe)_2SiO_4$ binary systems (Davidson and Mukhopadhyay, 1984). The value for ΔG^0_E was taken from Davidson and Mukhopadhyay.

Values determined for Pyx solution parameters are listed in Table 5, along with the values adopted from Davidson et al. (1988) for Fe-free Opx and Cpx. There are two qualitative differences from earlier values by Davidson and Lindsley (1985): (1) The temperature dependence of ΔG^0_2 (Opx) is smaller, as a result of including Ol + Opx + Q equilibria. This result was anticipated by Sack (1980) in his analysis of Ol + Opx exchange equilibria. (2) Nonzero values for W^{M1}_{Opx}, W^{M2}_{Opx}, and W^{M1}_{Cpx} are required by the expanded database used in the present analysis. For Opx, these values result in improved fits to cation-distribution and solution-enthalpy measurements relative to the 1985 model. For Cpx, calculated Pyx phase relations are similar to the 1985 model; however, Aug solvus limbs are displaced to slightly higher Ca contents.

Table 4. Olivine solution parameters

$\Delta G^0_2 = (7000.)$	$W_{23} = W_{32} = (21560.)$
$\Delta G^0_E = (-840.)$	
$W^{M1} = 0.$	$W_{13} = 34250. + 0.49P$
$W^{M2} = 0.$	$W_{31} = 30900. + 0.43P$

Note: Units are joules, bars, and kelvins. Values in parentheses were not determined with CMFS experiment; see text.

Table 5. Pyroxene solution parameters

Clinopyroxene	
$\Delta G^0_2 = -33489. + 27.9119T - 0.12518P$	$W_{23} = 20001 + 0.0271P$
$\Delta G^0_E = 5052.$	$W_{32} = 18682 - 0.0864P$
$W^{M1} = 3306.$	$W_{13} = 32301 - 0.00670P$
$W^{M2} = -2172.$	$W_{31} = 26125 - 0.03843P$
Orthopyroxene	
$\Delta G^0_2 = -15443. + 13.613T$	$W_{23} = W_{32} = 6000.$
$\Delta G^0_E = 13623.$	
$W^{M1} = 3514.$	$W_{13} = W_{31} = 20000.$
$W^{M2} = 5423.$	

Note: Units are joules, bars, and kelvins.

Our preferred apparent standard-state free-energy functions for Ol, Opx, and Cpx quadrilateral end-members and Q are given in Table 1. An important difference between this set and its predecessor by Helgeson et al. (1978) is the inclusion of coefficients of isothermal compressibility and isobaric thermal expansion for the quadrilateral end-members. We have incorporated measured values where available; sources are given in Table 1. Where unavailable, we have estimated them by assuming that quadrilateral end-member values are coplanar.

Model results and applications

A principal goal in developing this model is to provide tools for petrogenetic interpretation: geothermometry, geobarometry, and activity indicators for components such as SiO_2, $Fe_2Si_2O_6$, and Fe_2SiO_4. Table 6 summarizes various CMFS assemblages and necessary and/or desired analytical data that are most useful in constraining P, T, and a_i. For each assemblage, equilibrium requires that chemical-potential equalities of the form $\mu_{Mg_2Si_2O_6}$ in Aug $= \mu_{Mg_2Si_2O_6}$ in Opx and/or in Pig and/or in (Ol + Q) for Mg, Fe, and Ca components be met simultaneously. The variance indicates the minimum number of intensive variables needed to specify the conditions of equilibrium. Where desired data number more than the variance, the

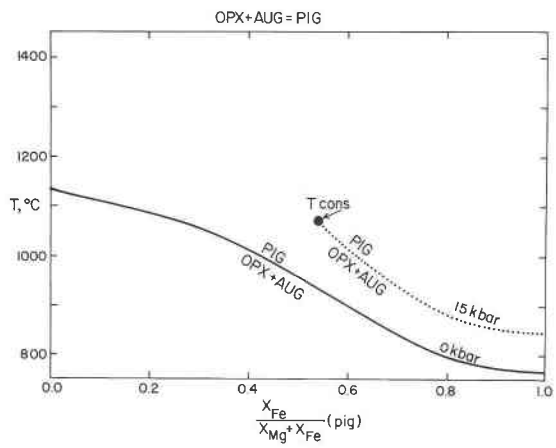

Fig. 6. T vs. Fe/(Fe + Mg) section for the reaction Opx + Aug = Pig, for 0 and 15 kbar. The 15-kbar reaction is truncated by the consolute point (T_{cons}) for Pig = Aug.

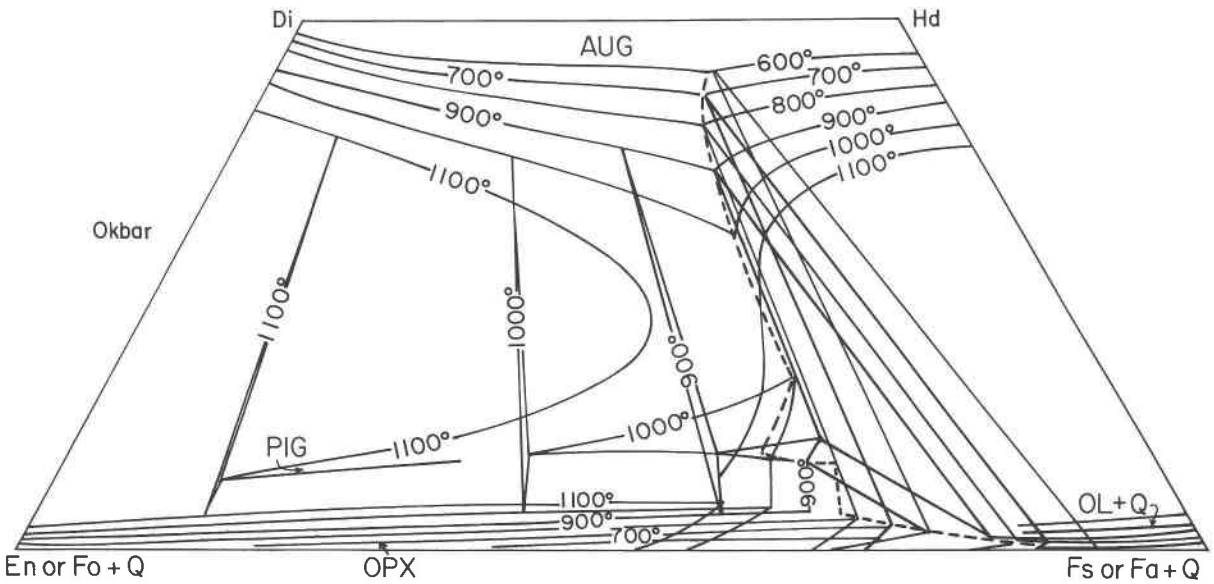

Fig. 7. Isotherms for 0-kbar phase relations among quadrilateral Pyx, Ol, and Q.

system is overdetermined; the desired intensive parameters can be optimized to available composition measurements. We are preparing an executable program (available on request from the authors) that calculates these properties on a PC. Calculated temperatures, pressures, and silica activities for key assemblages and conditions are shown graphically in Figures 6–12.

Several commonly used geothermometers are shown in Figures 6–8. Minimum temperatures vs. Fe/(Fe + Mg) ratio for Pig stability at several pressures are shown in Figure 6. Isotherms for bulk compositions in the pyroxene quadrilateral are shown here for both 0 kbar (Fig. 7) and 15 kbar (Fig. 8). Minor differences between these isotherms and those determined graphically by Lindsley (1983) result from the Ca contents of Aug saturated with low-Ca Pyx, which are calculated to be systematically higher for all but the Fe-free join. Therefore, the minimum temperature estimated for the stability of Aug of a given composition will be higher by our new model than by Lindsley's (1983) graphs.

Useful geobarometers are shown in Figures 9–11. The compositions of phases vs. P of the near-isothermal, univariant assemblage Aug + Opx + Pig + Ol + Q are plotted in Figure 9. Because the compositions of Aug, Opx, and Pig are almost collinear near the minimum temperature of 798 °C and ~6.5 kbar, we looked for, but did not find, a reversal in the relative Fe/(Fe + Mg) ratios of Pig vs. Aug + Opx. In any case, X_{Mg} of the terminally univariant Pig increases monotonically with pressure, producing a very good, temperature-independent geobarometer, as noted by Lindsley and Grover (1980). Our model defines this as P (in kbar) = 9.15 − 33.8 (X_{Mg}^{Pig}).

TABLE 6. Summary of model applications and required and/or desired analytical data

Type	Variance	Required and/or desired data	Result
		Geothermometers	
One-pyroxene (saturated or consolute)	3	X (=X_{Mg}), Y (=X_{Ca}), P	T_{Min} or T_{Max}; composition of second pyroxene
Two-pyroxene	3	X, Y (both phases)	T and (P)
Three-pyroxene	2	X, Y (all phases)	T and P
		Geobarometers	
Single low-Ca pyroxene (saturated)	3	X, Y (T; not sensitive)	P_{Min}
Olivine + quartz (Ol + Q) (saturated)	3	X, Y (T; not sensitive)	P_{Max}
Ol + Q + augite	3	X, Y (both phases)	P and (T)
Ol + Q + two pyroxenes	2	X, Y (all phases)	P and (T)
Ol + Q + three pyroxenes	1	X, Y (all phases)	P ($T \approx 820$ °C)
		Silica activity	
Olivine + one pyroxene	4	X, Y (olivine), P, T [or X, Y (both phases)]	a_{SiO_2}
Olivine + two pyroxenes	3	X, Y (all phases)	a_{SiO_2}

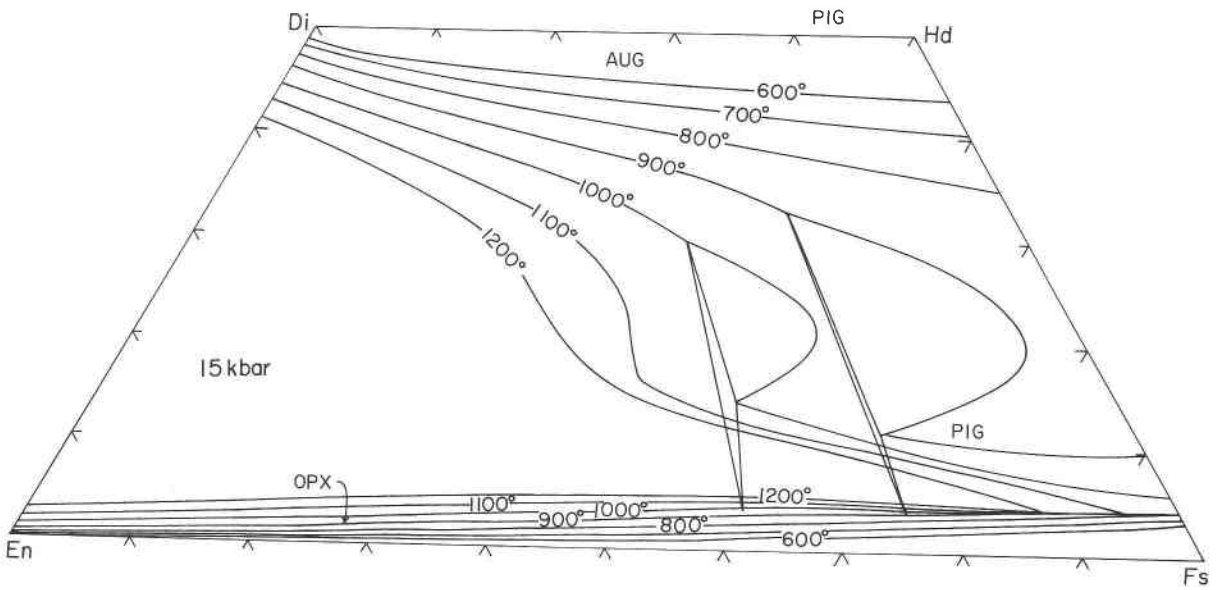

Fig. 8. Isotherms for 15-kbar phase relations among quadrilateral Pyx.

The Ol compositions coexisting with Q, Aug, and Opx are shown vs. P in Figure 10a. These indicate maximum pressures for which an Ol of the given composition is stable with Q. Corresponding isopleths of Opx, plotted in Figure 10b, show minimum pressures at which the low-Ca Pyx becomes stable. X_{Mg} values of Ca-bearing Opx saturated with Ol + Q + Aug are *lower* than their counterparts from the Ca-free system, so a minimum pressure determined from Figure 10b would be lower than that determined from comparison with Ca-free Opx equilibria. For the FMS system, model Opx + Ol + Q equilibria are shown on a P-T-X diagram in Figure 11.

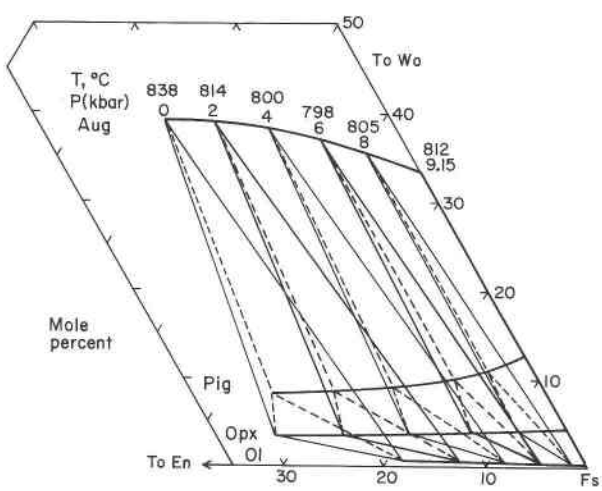

Fig. 9. Compositions and pressures for the five-phase assemblage Opx + Aug + Pig + Ol + Q. $T = 818 \pm 20$ °C.

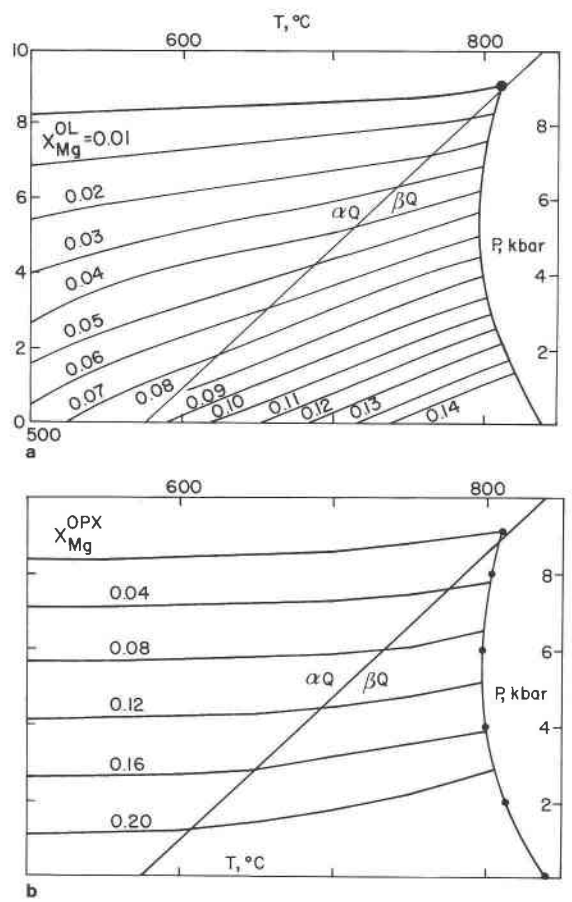

Fig. 10. Pyx + Ol + Q geobarometer. **(a)** Isopleths of X_{Mg} for Ol coexisting with Aug, Q, and Opx. **(b)** Isopleths of X_{Mg} for Opx coexisting with Aug, Ol, and Q.

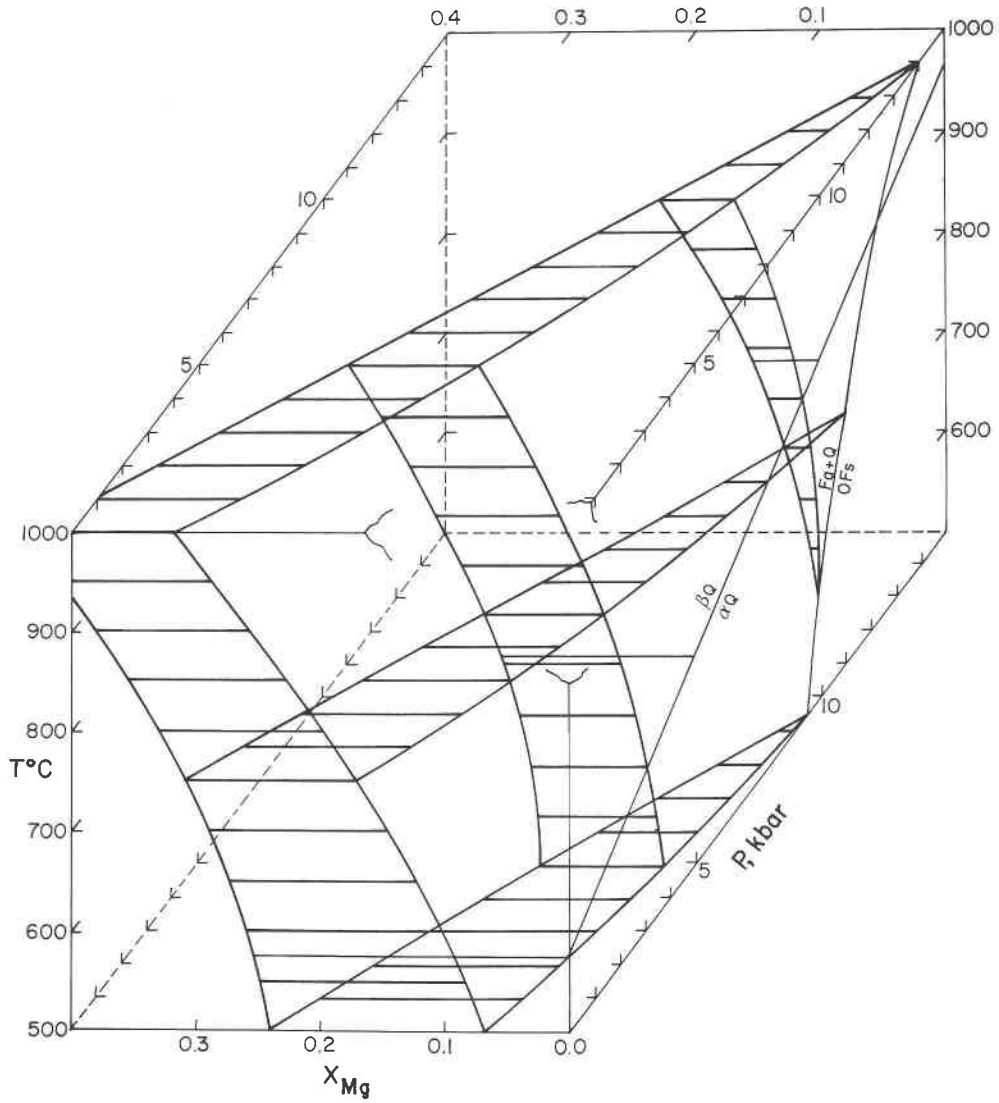

Fig. 11. P-T-X_{Mg} projection of Ca-free Ol + Q + Opx equilibria.

Silica activity

Exchange equilibria among Pyx and Ol at given P and T define the activity of a SiO_2 component (see Table 6). In the CMFS system, exchanges of Mg, Fe, *and* Ca take place between Pyx and Ol, and as a result, intensive parameters such as a_{SiO_2} are sensitive not only to P, T, and Fe/(Fe + Mg) ratios of the phases, but also to their Ca contents. Figure 12 shows calculated values for silica activity vs. X_{Mg} of Ol, from Opx-Ol and Cpx-Ol exchange equilibria. From Figure 12, it is apparent that silica activity increases with the relative stability of the Fe-rich Ol + Q assemblage, as indicated by (1) increasing Fe/(Fe + Mg) ratio, (2) decreasing pressure, (3) increasing temperature, and (4) decreasing Ca content. For the Opx-Ol exchange, the Fe/(Fe + Mg) ratio in Ol exerts dominant control over silica activity; pressure, temperature, and Ca content are of minor, subequal importance. For Cpx-Ol exchange, the surprising feature is the magnitude of the effect of Ol (and consequently, Cpx) Ca content on silica activity. These results suggest that it is critical to determine the complete Ol composition before attempting to use a model such as ours for determining silica activity.

Summary and conclusions

We have developed an internally consistent set of thermodynamic models for Pyx, Ol, and Q in the CMFS system. The models are based on Davidson's (1985) formulation for quadrilateral solution properties and were calibrated simultaneously with Opx cation distributions, Opx solution enthalpies, and phase equilibria for coexisting Pyx and coexisting Pyx + Ol + Q. We performed new experiments on Pyx + Ol + Q equilibria where critical for constraining our model.

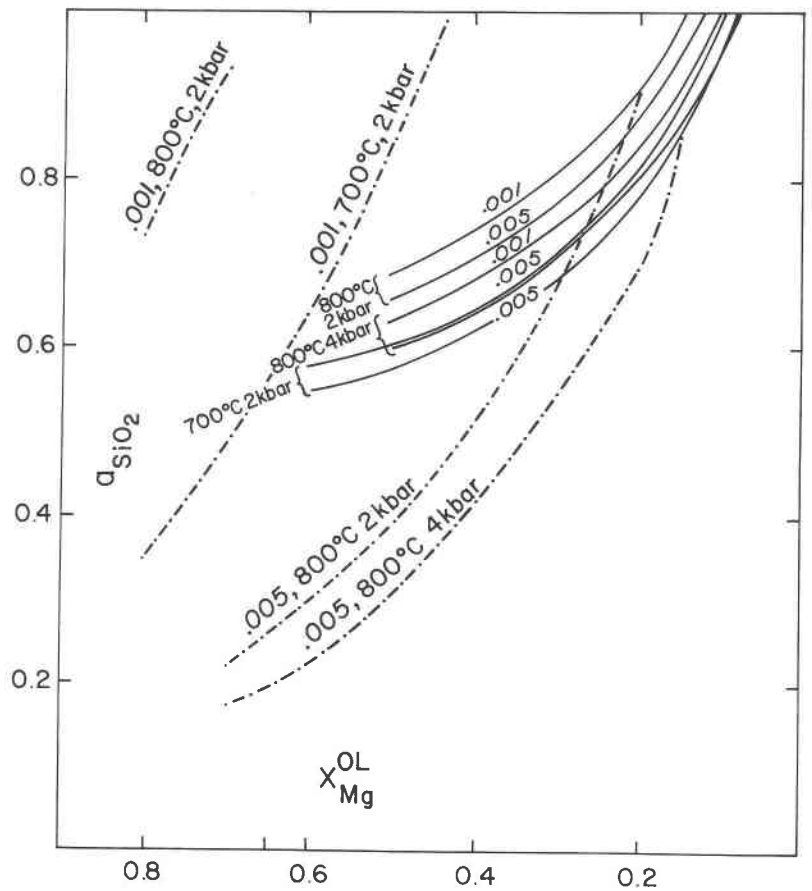

Fig. 12. Silica activity from Ol-Pyx exchange equilibria. Opx-Ol exchange is shown by solid curves; Cpx-Ol exchange by dash-dot curves. Ca contents of olivine are given with T and P.

Preferred values of model parameters (Tables 4 and 5) generate component activities that are consistent with our choice of apparent standard-state energies (Table 1). These values are modified from the compilation of Helgeson et al. (1978) to fit newer experimental data and to incorporate compressibility and thermal-expansion coefficients. Model component activities may not be consistent with other databases for standard-state energies unless energy differences among phases and among quadrilateral end-members are preserved.

Calculated thermometers include one-, two-, and three-Pyx equilibria. These differ topologically from those presented by Lindsley (1983) for 0 kbar because they include Carlson and Lindsley's (1988) model for Fe-free Pyx thermodynamics. Also, isothermal, isobaric Aug solvus limbs are displaced to higher Ca contents relative to Lindsley's graphical determinations. Calculated barometers include Ol + Q and one-, two-, or three-Pyx assemblages. The temperature for coexisting Ol + Q + Opx + Aug + Pig is 818 ± 20 °C, in agreement with Lindsley and Grover's (1980) experiments. Silica activity as determined from Ol-Pyx exchange equilibrium is shown to be a function not only of P, T, and Fe/(Fe + Mg) ratio of the assemblage, but of the Ol (and Pyx) Ca content as well. For Ol-Aug exchange equilibria, the Ca content in Ol may well exert the dominant control over silica activity and thus should be carefully analyzed in natural samples.

Acknowledgments

We thank John Grover for help with the unpublished experiments. We thank S. A. Morse and S. K. Saxena for their thorough, constructive reviews; however the authors bear sole responsibility for the interpretations and conclusions presented herein. Portions of the work were completed while P.M.D. held a National Research Council Associateship. Parts of this study were supported by NSF grants EAR 84-16254 and EAR 87-20185 to D. H. Lindsley.

References cited

Adams, G.E., and Bishop, F. (1982) Experimental investigation of Ca-Mg exchange between olivine, orthopyroxene and clinopyroxene: Potential for geobarometry. Earth and Planetary Science Letters, 57, 241–250.

——— (1985) An experimental investigation of thermodynamic mixing properties and unit-cell parameters of forsterite-monticellite solid solutions. American Mineralogist, 70, 714–722.

——— (1986) The olivine-clinopyroxene geobarometer: Experimental results in the CaO-FeO-MgO-SiO_2 system. Contributions to Mineralogy and Petrology, 94, 230–237.

Bass, J.D., and Weidner, D.J. (1984) Elasticity of single-crystal orthoferrosilite. Journal of Geophysical Research, 89, 4359–4371.

Besancon, J.R. (1981) Rate of cation disordering in orthopyroxenes. American Mineralogist, 66, 965–973.

Bohlen, S.R., and Boettcher, A.L. (1981) Experimental investigations and geological applications of orthopyroxene geobarometry. American Mineralogist, 66, 951–964.

Bohlen, S.R., Essene, E.J., and Boettcher, A.L. (1980) Reinvestigation and application of olivine-quartz-orthopyroxene barometry. Earth and Planetary Science Letters, 47, 1–10.

Brown, G.E., Prewitt, C.T., Papike, J.J., and Sueno, S. (1972) A comparison of the structures of low and high pigeonite. Journal of Geophysical Research, 77, 5778–5789.

Cameron, M., Sueno, S., Prewitt, C.T., and Papike, J.J. (1972) High-temperature crystal chemistry of acinite, diopside, hedenbergite, jadeite, spodumene, and ureyite. American Mineralogist, 58, 594–618.

Carlson, W.D. (1986a) Reversed pyroxene phase equilibria in CaO-MgO-SiO_2 from 925 to 1,175 °C at one atmosphere pressure. Contributions to Mineralogy and Petrology, 92, 218–224.

——— (1986b) Pigeonite phase equilibria at atmospheric pressure in CaO-MgO-SiO_2 (abs.). EOS, 67, 415.

Carlson, W.D., and Lindsley, D.H. (1988) Thermochemistry of pyroxenes on the join $Mg_2Si_2O_6$-$CaMgSi_2O_6$. American Mineralogist, 73, 242–252.

Chatillon-Colinet, C., Newton, R.C., Perkins, D.P., III, and Kleppa, O.J. (1983) Thermochemistry of $(Fe^{2+}, Mg)SiO_3$ orthopyroxene. Geochimica et Cosmochimica Acta, 47, 1597–1603.

Davidson, P.M. (1985) Thermodynamic analysis of quadrilateral pyroxenes. Part I: Derivation of the ternary nonconvergent site-disorder model. Contributions to Mineralogy and Petrology, 91, 383–389.

——— (1988) Phase separation in quadrilateral pyroxenes and olivines. In S. Ghose, Ed., Advances in physical geochemistry, 7, 39–59.

Davidson, P.M., and Lindsley, D.H. (1985) Thermodynamic analysis of quadrilateral pyroxenes. Part II: Model calibration from experiments and applications to geothermometry. Contributions to Mineralogy and Petrology, 91, 390–404.

Davidson, P.M., and Mukhopadhyay, D. (1984) (Ca,Mg,Fe) olivines: Experiments and a solution model. Contributions to Mineralogy and Petrology, 86, 256–263.

Davidson, P.M., Lindsley, D.H., and Carlson, W.D. (1988) Thermochemistry of pyroxenes on the join $Mg_2Si_2O_6$-$CaMgSi_2O_6$: A revision of the model for pressures up to 30 kbar. American Mineralogist, 73, 1264–1266.

Day, H.W., Chernosky, J.V., and Kumin, H.J. (1985) Equilibria in the system MgO-SiO_2-H_2O: A thermodynamic analysis. American Mineralogist, 70, 237–248.

Domeneghetti, M.C., Molin, O.M., and Tazzoli, V. (1985) Crystal-chemical implications of the Mg^{2+}-Fe^{2+} distribution in orthopyroxenes. American Mineralogist, 70, 987–995.

Dowty, E., and Lindsley, D.H. (1973) Mössbauer spectra of synthetic hedenbergite-ferrosilite pyroxenes. American Mineralogist, 58, 850–868.

Fonarev, V.I., and Graphchikov, A.A. (1982) Experimental study of Fe-Mg-Ca distribution between coexisting ortho- and clinopyroxenes at P = 294 MPa, T = 750 and 800 °C. Contributions to Mineralogy and Petrology, 79, 311–318.

Hazen, R.M. (1976) Effects of temperature and pressure on the crystal structure of forsterite. American Mineralogist, 61, 1280–1293.

Helgeson, H.C., Delany, J.M., Nesbit, H.W., and Bird, D.K. (1978) Summary and critique of the thermodynamic properties of rock-forming minerals. American Journal of Science, 278A, 1–229.

Holland, T.J.B., Navrotsky, A., and Newton, R.C. (1979) Thermodynamic parameters of $CaMgSi_2O_6$-$Mg_2Si_2O_6$ pyroxenes based on regular and cooperative disordering models. Contributions to Mineralogy and Petrology, 69, 337–344.

Kandelin, J., and Weidner, D.J. (1988) The elastic properties of hedenbergite. Journal of Geophysical Research, 93, 1063–1072.

Kretz, R. (1961) Some applications of thermodynamics to coexisting minerals of variable composition. Examples: Orthopyroxene-clinopyroxene and orthopyroxene-garnet. Journal of Geology, 69, 361–387.

Lager, G.A., and Meagher, E.P. (1978) High-temperature structural study of six olivines. American Mineralogist, 63, 365–377.

Levien, L., Weidner, D.J., and Prewitt, C.T. (1979) Elasticity of diopside. Physics and Chemistry of Minerals, 4, 105–113.

Lindsley, D.H. (1983) Pyroxene thermometry. American Mineralogist, 68, 477–493.

Lindsley, D.H., and Andersen, D.J. (1983) A two-pyroxene thermometer. Proceedings of the 13th Lunar and Planetary Sciences Conference, Journal of Geophysical Research Supplement, 88, A887–A906.

Lindsley, D.H., and Dixon, S.A. (1976) Diopside-enstatite equilibria at 850 to 1400 °C, 5–35 kbar. American Journal of Science, 276, 1285–1301.

Lindsley, D.H., and Grover, J.E. (1980) Fe-rich pigeonite: A geobarometer. Geological Society of America Abstracts with Programs, 12, 472.

Lindsley, D.H., and Munoz, J.L. (1969) Subsolidus relations along the join hedenbergite-ferrosilite. American Journal of Science, 276A, 295–324.

Lindsley, D.H., Grover, J.E., and Davidson, P.M. (1981) The thermodynamics of the $Mg_2Si_2O_6$-$CaMgSi_2O_6$ join: A review and an improved model. In R.C. Newton, A. Navrotsky, and B.J. Wood, Thermodynamics of minerals and melts, p. 149–176. Springer-Verlag, New York.

McCallister, R.H., Finger, L.W., and Ohashi, Y. (1976) Intracrystalline Fe^{2+}-Mg equilibria in three natural Ca-rich clinopyroxenes. American Mineralogist, 61, 671–676.

Mori, T. (1978) Experimental study of pyroxene equilibria in the system CaO-MgO-FeO-SiO_2. Journal of Petrology, 19, 45–65.

Mori, T., and Green, D.H. (1975) Pyroxenes in the system $Mg_2Si_2O_6$-$CaMgSi_2O_6$ at high pressure. Earth and Planetary Science Letters, 26, 277–286.

——— (1976) Subsolidus equilibria between pyroxenes in the CaO-MgO-SiO_2 system at high pressures and temperatures. American Mineralogist, 61, 616–625.

Mukhopadhyay, D.K., and Lindsley, D.H. (1983) Phase relations in the join kirschteinite ($CaFeSiO_4$)-fayalite (Fe_2SiO_4). American Mineralogist, 68, 1089–1094.

Nehru, C.E., and Wyllie, P.J. (1974) Electron microprobe measurement of pyroxenes coexisting with H_2O-undersaturated liquid in the join $CaMgSi_2O_6$-$Mg_2Si_2O_6$-H_2O at 30 kilobars, with applications to geothermometry. Contributions to Mineralogy and Petrology, 48, 221–228.

Nickel, K.G., and Brey, G. (1984) Subsolidus orthopyroxene-clinopyroxene systematics in the system CaO-MgO-SiO_2 to 60 kb: A re-evaluation of the regular solution model. Contributions to Mineralogy and Petrology, 87, 35–42.

Podpora, C., and Lindsley, D.H. (1979) Fe-rich pigeonites: Minimum temperatures of stability in the Ca-Mg-Fe quadrilateral (abs.). EOS, 60, 420–421.

Ramberg, H., and Devore, G. (1951) The distribution of Fe^{++} and Mg^{++} in coexisting olivines and pyroxenes. Journal of Geology, 59, 193–210.

Robie, R.A., Finch, C.B., and Hemingway, B.S. (1982) Heat capacity and entropy of fayalite (Fe_2SiO_4) between 5.1 and 383 K: Comparison of calorimetric and equilibrium values for the QFM buffer reaction. American Mineralogist, 67, 463–469.

Sack, R.O. (1980) Some constraints on the thermodynamic mixing properties of Fe-Mg orthopyroxenes and olivines. Contributions to Mineralogy and Petrology, 71, 257–269.

Saxena, S.K., and Ghose, S. (1971) Mg^{2+}-Fe^{2+} order-disorder and the thermodynamics of the orthopyroxene solution. American Mineralogist, 56, 532–559.

Saxena, S.K., and Nehru, C.E. (1975) Enstatite-diopside solvus and geothermometry. Contributions to Mineralogy and Petrology, 49, 259–267.

Saxena, S.K., Ghose, S., and Turnock, A.C. (1974) Cation distribution in low-calcium pyroxenes: Dependence on temperature and calcium content and the thermal history of lunar and terrestrial pigeonites. Earth and Planetary Science Letters, 21, 194–200.

Schweitzer, E. (1982) The reaction pigeonite = diopside_{ss} + enstatite_{ss} at 15 kbar. American Mineralogist, 67, 54–58.

Smyth, J.R. (1973) An orthopyroxene structure up to 850 °C. American Mineralogist, 58, 636–648.

Sueno, S., Cameron, M., and Prewitt, C.T. (1976) Orthoferrosilite: High-temperature crystal chemistry. American Mineralogist, 61, 38–53.

Sykes, J., and Molin, G.M. (1986) Structural variations in orthopyroxenes (abs.). Proceedings of the 14th Meeting of the International Mineralogical Association, 243.

Thompson, J.B., Jr. (1969) Chemical reactions in crystals. American Mineralogist, 54, 341–375.

——— (1970) Chemical reactions in crystals: Corrections and clarifications. American Mineralogist, 55, 528–532.

Turnock, A.C., and Lindsley, D.H. (1981) Experimental determination of pyroxene solvi for P <= 1 kb, 900 °C and 1000 °C. Canadian Mineralogist, 19, 225–267.

Warner, R.D., and Luth, W.C. (1974) The diopside-orthoenstatite two-phase region in the system $CaSiO_3$-$FeSiO_3$-$MgSiO_3$. American Mineralogist, 59, 98–109.

Weidner, D.J., and Vaughan, M.T. (1982) Elasticity of pyroxenes: Effects of composition versus crystal structure. Journal of Geophysical Research, 87, 9349–9353.

Wells, P.R.A. (1977) Pyroxene thermometry in simple and complex systems. Contributions to Mineralogy and Petrology, 62, 129–139.

Wood, B.J., and Banno, S. (1973) Garnet-orthopyroxene and orthopyroxene-clinopyroxene relationships in simple and complex systems. Contributions to Mineralogy and Petrology, 42, 109–124.

Wood, B.J., and Kleppa, O.J. (1981) Thermochemistry of forsterite-fayalite olivine solutions. Geochimica et Cosmochimica Acta, 45, 529–534.

Yagi, T., Ida, Y., and Akimoto, S. (1975) Effect of hydrostatic pressure on the lattice parameters of Fe_2SiO_4 olivine up to 70 kbar. Physics of the Earth and Planetary Interiors, 10, 348–354.

Manuscript received December 1, 1987
Manuscript accepted September 30, 1988